Environ Sci Pollut Res (2018) 25:2830–2841
https://doi.org/10.1007/s11356-017-0500-6

RESEARCH ARTICLE

Combining stable carbon isotope analysis and petroleum-fingerprinting to evaluate petroleum contamination in the Yanchang oilfield located on loess plateau in China

Yiping Wang[1] · **Jidong Liang**[1,2] · **Jinxing Wang**[1] · **Sha Gao**[1,3]

Received: 23 April 2017 / Accepted: 17 October 2017 / Published online: 15 November 2017

Abstract This study evaluated petroleum contamination in the Yanchang (Shaanxi Yanchang Petroleum (Group) Co., Ltd.) oilfield, located in the loess plateau region of northern Shaanxi, China. Surface soil and sediment samples were collected from the wasteland, farmland, and riverbed in this area to assess the following parameters: total petroleum hydrocarbon (TPH), n-alkanes, polycyclic aromatic hydrocarbons (PAHs), and carbon isotope ratios (δ^{13}C). The results showed that TPH and PAH levels in the study area were 907–3447 mg/kg and 103.59–563.50 μg/kg, respectively, significantly higher than the control samples (TPH 224 mg/kg, PAHs below method quantification limit, MQL). Tests using δ^{13}C to detect modified TPH (2238.66 to 6639.42 mg/kg) in the wastelands adjacent to the oil wells revealed more significant contamination than tests using extraction gravimetric analysis. In addition, "chemical fingerprint" indicators, such as low to high molecular weight (LMW/HMW) hydrocarbons, carbon preference index (CPI), and pristine/phytane (Pr/Ph), further confirmed the presence of heavy petroleum contamination and weathering. This has resulted in a nutrient imbalance and unsuitable pH and moisture conditions for microbial metabolic activities. This study evaluates petroleum contamination, which can inform contamination remediation on a case by case basis.

Keywords Total petroleum hydrocarbon (TPH) · N-alkanes · Polycyclic aromatic hydrocarbons (PAHs) · Carbon isotope ratios (δ^{13}C) · Loess

Introduction

The Yanchang oilfield is located in the loess plateau region in the northern part of Shaanxi, China. In the past 20 years, petroleum production from this field has increased rapidly, from one million tons to more than 12 million tons per year. Yanchang has become one of the most important energy production bases in China. Unfortunately, environmental pollution has accompanied this petroleum extraction, leading to the accumulation of persistent petroleum compounds in the environment. Further, soil erosion is a serious problem in the Loess Plateau, due to its fragile ecosystem. As a result, contaminated soils can become a pollution source, allowing contaminants to spread on a large scale. There have been few reports about petroleum contamination in this area. Therefore, petroleum pollution investigations are needed to drive prompt risk management and petroleum contamination remediation.

Petroleum is a complex mixture, composed of alkanes, aromatics, resins, asphaltenes, and other organic matter (Salanitro et al. 1997). Some petroleum compounds are known to have carcinogenic, mutagenic, and teratogenic effects. As such, many countries have classified petroleum as a type of hazardous compound (Huang et al. 2016, Zhou et al.

Responsible editor: Zhihong Xu

Electronic supplementary material The online version of this article (https://doi.org/10.1007/s11356-017-0500-6) contains supplementary material, which is available to authorized users.

✉ Jidong Liang
jidongl@mail.xjtu.edu.cn

[1] Department of Environmental Engineering, Xi'an Jiaotong University, Xi'an 710049, China

[2] State Key Laboratory of Loess and Quaternary Geology, Institute of Earth Environment, Chinese Academy of Sciences, Xi'an 710061, China

[3] Department of Environmental Science, Chang'an University, Xi'an 710054, China

2011). Petroleum and its derivatives are released into the environment during petroleum extraction, storage, transportation, and production processes. They enter plants and animals through the food chain, further threatening the ecosystem and human health.

Previous investigations have indicated that petroleum residue concentrations in the heavily contaminated area of an oilfield can reach 4–20%, or 50–1000 times greater than the environmental background value (Liang et al. 2012). Petroleum composition significantly changes after a long natural attenuation period in soil ecosystems, but it is difficult to evaluate these changes (Quatrini et al. 2008; Shi et al. 2017). After the petroleum is released into the environment, its components degrade significantly as a result of physical, chemical, and biological factors. The biodegradation is believed to dominate the long-term residual degradation process (Nocentini et al. 2000).

Petroleum biodegradation involves two main processes: anabolism and catabolism. Some petroleum is transformed into a microbial biomass, and some is completely mineralized into carbon dioxide (CO_2) and water (H_2O). However, some organic exometabolites cannot be used by microorganisms, and remain as persistent organic pollutants. Of the petroleum components, n-alkenes are considered the most easily biodegradable compounds, while polar components are more resistant to biodegradation. As a result, polar components contain resin and asphaltene that accumulated in the environment (Atlas and Hazen 2011).

A powerful analysis tool is needed to assess the level of petroleum contamination, attenuation, and accumulation in the environment. Petroleum-fingerprinting provides information about the source and extent of petroleum degradation using gas chromatography/mass spectrometry (GC/MS). This tool analyzes the characteristic components identified in the petroleum (Douglas et al. 1996; Wang et al. 2012). For example, n-alkane distribution indices, carbon preference index (CPI), n-C_{17}/pristane (Pr), and n-C_{18}/phytane (Ph) are used to indicate biogenic and petrogenic sources of petroleum and their degradation processes (Gao et al. 2007; Tran et al. 1997; Zheng and Richardson 1999). N-alkanes and PAH concentrations can be used to assess contamination levels (Teng et al. 2015). All of these parameters are analyzed after extracting the samples using special solvents; as a result, non-extractable petroleum fractions are not included in the determination. Ziakun et al. (2014) reported that the ratio of stable carbon isotope distribution ($^{13}C/^{12}C$) in the organic carbon of petroleum differs from the ratio in uncontaminated soil. Thus, it can be used as a natural isotope to quantify non-extractable petroleum residues.

This study investigated petroleum contamination in the loess of the Yanchang oilfield, using a combination of petroleum-fingerprinting and stable carbon isotope analysis. Surface soil and sediment samples were collected from wasteland, farmland, and riverbed areas, and samples were analyzed for TPH, n-alkane, PAH, and $\delta^{13}C$ levels, and physiochemical properties. Furthermore, modified TPHs in the wasteland were detected using stable carbon isotope analysis, and petroleum-fingerprinting assessed the attenuation and accumulation of different components in the loess. This work offers important background information to inform petroleum pollution remediation in this area.

Materials and methods

Sampling site background

The sampling sites were located in the Yan River drainage area in the loess plateau region of northern Shaanxi, China. This region has a semi-arid continental climate, with an average annual precipitation of 470 mm. Most of the rain falls in June and September. The average annual temperature ranges from 7.87 to 10.60 °C. The soil type is classified as typical loessal soil, which is easily eroded, causing nutrient deficiency. Vegetative coverage is sparse in this area, due to the climatic conditions and geological characteristics.

Sample collection and preparation

The study was conducted in October 2015. Table 1 describes the sample sites with serial numbers, locations, and durations of oil wells. The samples identified as O-1 to O-5 came from wasteland sampling sites, adjacent to active oil wells. Samples N-6 and N-7 came from wasteland sampling sites adjacent to waste oil wells. Samples F-8 and F-9 came from the corn and radish farmland. Samples S-10 to S-13 came from the riverbed of the Yan River, which flows through the Yanchang oilfield. Uncontaminated soil samples were collected from an undisturbed area in this region, and were used as a background reference.

Each surface soil sample was collected from the same depth (0–10 cm) and consisted of a homogeneous mixture of five subsamples collected on a diagonal at each site. Samples were stored in sterilized bags, transported to the laboratory, and refrigerated at 4 °C prior to experimental analysis. Before analysis, samples were air-dried at room temperature, and were passed through an 80-mesh sieve to remove large particles.

Analysis methods

Physiochemical properties of soil and sediment

The pH values of the samples were analyzed using a pH meter (OHAUS ST2100/3C Pro-B, USA) in a soil and deionized water suspension (1:2.5 soil weight/water volume). Total

Table 1 Basic information of the sampling sites in Yanchang oilfield, China

Sample no.	Type of sample	Detail information of the sampling sites	Geographic coordinate	
			Latitude (N)	Longitude (E)
O-1	Soil	Wasteland adjacent to Liujiagou Oilwell (1992–2015)	36° 41′ 21.23″	109° 41′ 54.26″
O-2		Wasteland adjacent to Pianqiao Oilwell (2000–2015)	36° 38′ 39.70″	109° 41′ 40.01″
O-3		Wasteland adjacent to Fengfuchuan Oilwell (2007–2015)	36° 40′ 19.42″	109° 38′ 34.96″
O-4		Wasteland adjacent to Nanniwan Oilwell (2010–2015)	36° 35′ 31.98″	109° 36′ 37.44″
O-5		Wasteland adjacent to Xiatonggou Oilwell (2015–)	36° 42′ 04.85″	109° 35′ 53.10″
N-6		Wasteland adjacent to Nanniwan Oilwell (1987–2014)	36° 32′ 04.30″	109° 32′ 23.67″
N-7		Wasteland adjacent to Xiatonggou Oilwell (1992–2004)	36° 41′ 30.13″	109° 41′ 54.26″
FL-8	Soil	Farmland with corn, near to Fengfuchuan Oilwell (2007–2015)	36° 41′ 06.75″	109° 35′ 33.10″
FL-9		Farmland with radish, near the Nanniwan Oilwell (1987–2014)	36° 33′ 18.30″	109° 32′ 28.67″
S-10	Sediment	Yanhe Riverbed, near to Fengfuchuan Oilwell (2007–2015)	36° 40′ 44.75″	109° 40′ 10.94″
S-11		Yanhe Riverbed, near to Xiantonggou oil-wastewater treatment plant	36° 37′ 40.49″	109° 32′ 33.09″
S-12		Yanhe Riverbed, near to Yaodian wastewater treatment plant	36° 44′ 42.25″	109° 32′ 35.10″
S-13		Yanhe Riverbed, near to abandon of Xiatonggou Oilwell (2015–)	36° 32′ 04.30″	109° 41′ 54.26″
P-14	Petroleum	Dominated by Yanchang Oilfield, Yan'an, Northern Shaanxi, China	36° 41′ 04.65″	109° 37′ 54.10″
B-15	Soil	Wasteland lack of vegetation and far from the oil wells	36° 48′ 03.30″	109° 54′ 34.16″

organic carbon (TOC) was determined using the potassium dichromate dilution heat colorimetric method (Karvelas et al. 2003). Total nitrogen (TN) was analyzed using the Kjeldahl method. Total phosphorous (TP) was measured colorimetrically as molybdovanadate phosphoric acid (Wang et al. 2010). Gravimetric moisture was measured after drying the soil at 105 °C for 24 h (Koponen et al. 2006).

TPH, saturates, aromatics, and polar components

An aliquot (ca. 5 g) of each sample was extracted with 20 mL dichloromethane using ultrasonication for 15 min; the extract was then centrifuged for 10 min at 4000 r/min. This procedure was repeated three times to generate the final petroleum hydrocarbon extract. Half of the extract was concentrated into a dry substance, using a rotary evaporator at 40 °C. The TPH level was then determined gravimetrically. The other half of the extract was separated into saturates, aromatics, and polar components using column chromatography with a silica gel alumina column (30 cm × 10 mm i.d). Saturated and aromatic fractions were eluted with n-hexane and n-hexane/DCM (1:1 *v*/*v*), respectively; saturated, aromatic, and polar component levels were then determined gravimetrically.

N-alkenes and PAHs

The separate saturated fractions generated by the process above were analyzed using an Agilent 6890 GC, with a HP-5 fused silica capillary column (30 m × 0.25 mm i.d. × 0.25-mm-thick film) connected to an Agilent 5973 mass selective detector to obtain information about n-alkanes. The GC oven temperature was programmed as follows: 70 °C for 1 min, followed by a temperature increase of 4 °C/min to an increase of 300 °C, held for 5 min. The injector and interface temperature was set at 280 °C. An *m*/*z* 57 was used to determine aliphatic hydrocarbons. Peak levels of individual alkanes were used to determine their respective concentrations in the samples. Quantification was performed using external hydrocarbon mixture standards, ranging from n-C_8 to n-C_{40}.

Similarly, the aromatic fractions were separated as described above; 16 PAHs identified by the US Environmental Protection Agency (USEPA) (Havelcova et al. 2014) were analyzed using an Agilent 6890 GC with a HP-5 fused silica capillary column (30 m × 0.25 mm i.d. × 0.25 mm film thickness), connected to an Agilent 5973 mass selective detector. The GC oven temperature was programmed as follows: 60 °C for 2 min, followed by a temperature increase of 3 °C/min to 290 °C, held for 5 min. The PAHs were determined using selected ion monitoring (SIM). SIM acquisition was carried out by comparing the base peak of each PAH.

Organic carbon isotope ($\delta^{13}C$) analysis

Organic carbon isotope ratios ($\delta^{13}C$) of the samples were measured using a MAT 251 gas mass spectrometer (Thermo Finnigan, Germany) with a dual inlet system. Approximately 2 g of each sample was combusted for 4 h at 850 °C in a vacuum-sealed quartz tube in the presence of Pt, cupric oxide, and copper. The CO_2 gas was extracted and cryogenically purified, and the isotope composition of the extracted CO_2 gas was then analyzed. A routine laboratory work standard with a known $\delta^{13}C$ value was also measured each day. The analytical precision with the standards (MAT 251) was 0.2‰. The quantitative levels of ^{13}C and ^{12}C isotopes in specimens were characterized using a ratio of peak intensities of m/z 45 ($^{13}C^{16}O_2$) and 44 ($^{12}C^{16}O_2$) in the mass spectrum of CO_2. The amounts of carbon isotope ^{13}C were measured in relative units ($\delta^{13}C$, ‰):

$$\delta^{13}C = (R_{sa}/R_{st}-1) \times 1000‰ \quad (1)$$

In this expression, $R_{sa} = (^{13}C)/(^{12}C)$ was the $^{13}C/^{12}C$ isotope distribution ratio determined for the specimen, and $R_{st} = (^{13}C)/(^{12}C)$ was the same ratio for the Pee Dee Belemnite international standard. Each CO_2 specimen was analyzed in three replicates; the standard error was ± 0.1‰.

Statistical analysis

Statistical analyses were performed using SPSS version 19.0 for Windows (SPSS, Germany). The Pearson correlation coefficient (r) was calculated to determine the relationship between soil physiochemical parameters and TPH.

Results and discussion

Petroleum contamination and the environmental impact

Concentration of TPH

Analysis of variance (ANOVA) showed that the TPH concentrations in different samples were significantly different ($p < 0.05$). Table 2 shows that TPH concentrations (1607–3447 mg/kg) were 7.27–14.45 times higher in the wasteland adjacent to seven oil wells than in the uncontaminated soil (224 mg/kg). The levels were significantly higher than the local soil safety limit (500 mg/kg). The loess plateau in north Shaanxi has a temperate continental monsoon climate with a mean annual rainfall of 470 mm. The natural vegetation is sparse, the ecosystem is fragile, and soil erosion is common. As such, contaminants spread as the soil erodes, leading to a wider area of petroleum pollution. This study found that TPH concentrations in the farmland and river sediment were 800–1000 and 1400–2200 mg/kg, respectively. These values are significantly higher than background values (224 mg/kg) (Table 2). Liang et al. (2012) reported TPH concentrations of 700–4000 mg/kg in the loess plateau region (34° 20′ N, 107° 10′ E), similar to TPH pollution levels in this study.

In short, the soil and river in the Yanchang oilfield in northern Shaanxi of China were found to be significantly contaminated by petroleum. Oil wells in the Yanchang oilfield dot the farming area, creating significant potential hazards for human beings from widespread petroleum contamination. Many studies have shown that petroleum contamination leads to short- or long-term acute or chronic toxic effects on human and ecosystem health (Labud et al. 2007; Peng et al. 2009). Thus, effectively controlling or remediating petroleum pollution at specific sites is critical.

Composition of saturates, aromatics, and polar components

In general, the residual petroleum in soil were composed of saturates, aromatics, and polar component fractions (i.e., resins and asphaltenes).The percentage levels of saturates, aromatics, and polar components among seven wasteland soils

Table 2 TPH concentration and physiochemical properties of the samples collected in Yanchang oilfield, Northern Shaanxi, China

Sample no.	TPH (mg/kg)	TOC (g/kg)	pH	Moisture (%)	TN (g/kg)	TP (g/kg)	C/N	C/P
B-15[a]	224 ± 30.33	5.07 ± 1.11	8.71 ± 0.21	9.33 ± 2.33	0.44 ± 0.07	1.07 ± 0.24	11.52	4.74
O-1	1607 ± 149.93	7.24 ± 2.07	8.36 ± 0.33	8.42 ± 2.43	0.35 ± 0.10	1.05 ± 0.22	20.69	6.90
O-2	2153 ± 143.80	7.56 ± 2.38	8.31 ± 0.29	11.61 ± 3.21	0.37 ± 0.18	0.99 ± 0.31	20.43	7.64
O-3	2593 ± 177.67	7.92 ± 3.01	8.26 ± 0.18	11.22 ± 2.57	0.37 ± 0.05	0.94 ± 0.11	21.41	8.43
O-4	3447 ± 203.45	9.79 ± 3.76	8.18 ± 0.40	13.43 ± 2.11	0.30 ± 0.07	0.94 ± 0.30	32.63	10.41
O-5	1733 ± 113.67	6.26 ± 1.18	8.50 ± 0.20	9.07 ± 3.47	0.33 ± 0.07	0.86 ± 0.10	18.97	7.28
N-6	2080 ± 129.87	7.52 ± 2.01	8.25 ± 0.19	3.01 ± 1.61	0.39 ± 0.08	0.89 ± 0.12	19.28	8.45
N-7	1780 ± 101.55	8.58 ± 1.78	8.37 ± 0.21	14.64 ± 3.87	0.41 ± 0.11	0.81 ± 0.27	20.93	10.59
FL-8	907 ± 77.86	9.55 ± 2.39	8.99 ± 0.31	23.08 ± 4.07	1.82 ± 0.18	3.07 ± 0.51	5.25	3.11
FL-9	1027 ± 67.87	9.85 ± 1.76	9.01 ± 0.33	20.91 ± 5.21	2.05 ± 0.29	3.22 ± 0.49	4.80	3.06
S-10	1993 ± 133.47	9.33 ± 1.01	8.21 ± 0.42	57.91 ± 8.49	0.44 ± 0.06	0.97 ± 0.10	21.20	9.61
S-11	1540 ± 124.56	5.91 ± 1.77	8.58 ± 0.25	50.17 ± 9.21	0.32 ± 0.07	0.98 ± 0.12	18.46	6.03
S-12	2287 ± 187.79	12.81 ± 2.87	8.02 ± 0.32	20.91 ± 5.29	0.67 ± 0.06	1.33 ± 0.33	19.12	9.63
S-13	1860 ± 167.77	10.33 ± 3.40	8.47 ± 0.27	57.91 ± 9.01	0.58 ± 0.14	2.34 ± 0.38	17.81	4.41

[a] B-15 as uncontaminated soil sample can be used as background reference. The data are average values ($n = 5$) with standard deviations

adjacent to the oil wells were significantly different ($p < 0.05$). Figure 1 shows that saturates were the main component, accounting for more than 50% of the total petroleum residues in all contaminated soils. Variations in the residual petroleum composition showed that the saturated hydrocarbon fraction gradually decreased from 79.67% (O-5, 2015–) to 62.24% (N-6, 1987–2014) as the duration of oil well use lengthened (older wells had a smaller saturated hydrocarbon fraction). However, polar component fractions significantly accumulated in the soil, from 5.03% (O-5, 2015–) to 13.68% (N-6, 1987–2014) over the duration of oil well use. In addition, the aromatic fractions accumulated slightly, with an average value of 21.49% in the contaminated soil, compared with the fraction in the petroleum (16.59%).

Different petroleum components showed different weathering behaviors. The saturates were the main component of the total petroleum residues in the wasteland adjacent to the oil wells; their concentration gradually decreased as the age of the oil wells increased. Aromatics and polar components accumulated as the age of the oil wells in the wasteland sites increased. Polar components accumulated more rapidly than the PAHs did. Some studies have found that saturated hydrocarbons are easily degraded, followed by aromatic hydrocarbons. In contrast, the stability of polar compounds makes them recalcitrant toward degradation (Atlas and Hazen 2011).

Our results are consistent with these references, as natural attenuation of petroleum occurred in each location, resulting in partial saturate removal. Polar components persist in the environment, leading to their accumulation over time as contamination continues. Fedorak and Westlake (1981) noted that increases in polar compounds in soil may result from the generation of polar biological metabolites during biodegradation. Thus, both recalcitrant polar components in petroleum, and polar biological metabolites from petroleum biodegradation, contribute to the accumulation of these compounds.

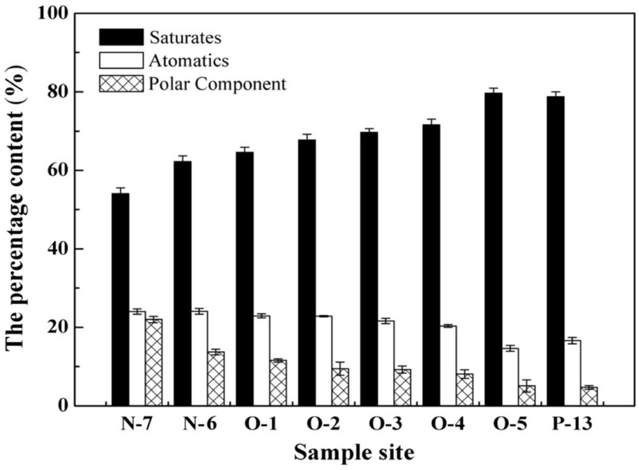

Fig. 1 Percentage content of saturates, aromatics, and polar components in the wasteland soil adjacent to oil wells

Physiochemical properties of soil affected by petroleum pollution

Weathered oil residues that have been present in soil for long periods may cause changes in soil physiochemical properties, impacting soil quality (Sarkar et al. 2005). Characterizing oil-contaminated soil is a crucial step in remediating it (Mao et al. 2009). Table 2 lists the TPH concentrations and physiochemical characteristics for the soil and river sediment in the Yanchang oilfield. The samples collected from the wasteland adjacent to oil wells contained significantly ($p < 0.05$) higher TPH concentrations (1607–3447 mg/kg) and TOC (6.26–9.79 g/kg) than the uncontaminated soil (TPH concentration of 224 mg/kg; TOC concentration of 5.07 g/kg). In contrast, TP and TN in the contaminated soil samples were slightly lower than the background soil. This increased the C/N (18.97–32.63) and C/P (6.90–10.59) ratios of the contaminated samples compared to the background samples ($C/N = 11.52$, $C/P = 4.74$). In addition, the pH of the contaminated soil (8.18–8.50) was slightly lower than in background samples (8.71).

The study area is located in the drought/semi-drought loess plateau; as such, all the wasteland soil samples had a relatively low moisture level, with an average value of 10.09%. In contrast to the wasteland, the farmland samples had only slight TPH contamination, at concentrations of 800–1000 mg/kg. Crops grow in this area. As such, organic carbon, N, and P inputs from plants lead to higher TOC (9.55–9.85 g/kg), TN (1.82–2.05 g/kg), and TP (3.07–3.22 g/kg) in the soil than seen in the wastelands. The pH levels in the farmland samples were slightly higher than in the wastelands, and the moisture levels were significantly higher than the background levels. River sediments were also contaminated with petroleum, with TPH concentrations of 1540–2287 mg/kg. In contrast with the soil samples, the pH values of the sediment samples were nearly neutral.

TOC contains all forms of organic carbon, including petroleum hydrocarbons and other natural organic matter from plant or microbial biomass (Wang et al. 2013). This study found that the TOC values in the contaminated soils were significantly ($p < 0.05$) higher than in the uncontaminated background soil. TOC was significantly ($p < 0.05$) positively correlated ($r = 0.771$) with TPH (Table S4) in the soil samples adjacent to the oil wells. Hence, the higher TOC at the contaminated sites may be due to petroleum input. This result is consistent with other studies (Wang et al. 2010). Gianfreda et al. (2005) found that organic carbon can be mostly attributed to the presence of organic waste, rather than organic biomass in the soils polluted by petroleum.

The pH value is a significant variable in soils because it impacts many chemical and biological processes. Previous studies have found that the optimal soil pH to biodegrade hydrocarbon contaminants in soils is 7.0–7.8 (Liang et al.

2012). However, the pH of this study's investigation area was alkaline (ranging from 8.18–8.71). Although the pH of the contaminated soil was slightly lower than background values, the values remained alkaline. This finding aligns with Liang et al. (2012), who reported that soils in most oil fields in northern China are alkaline, with decreased pH values observed in petroleum-contaminated soils.

In this study, pH was significantly ($p < 0.05$) negatively correlated with TPH ($r = -0.795$) and TOC ($r = -0.758$) (Table S4). This correlation may be due to the microbiodegradation of petroleum. In the biodegradation process, microorganisms produce carboxylic acid intermediates, which decrease soil pH (Leahy and Colwell 1990). There are, however, conflicting studies that found a significant increase in pH in crude oil-contaminated soil (Bauder et al. 2005). Chemical reactions between petroleum and soil elements may cause this variation in pH (Sun and Zhou 2007). Lauber et al. (2009)) highlighted that pH changes in the soil caused by petroleum contamination might affect the soil's physiochemical and biological properties, inhibiting microbial metabolic activities outside the optimal pH range. As such, assessing pH values in oil-contaminated soil is critical in evaluating remediation techniques.

Nitrogen and phosphorus levels in soil indicate soil fertility, which influences the microbial degradation of petroleum. In the petroleum-contaminated sites, TPH can increase the carbon levels in soil, influencing nutrient equilibrium (Braddock et al. 1997; Wang et al. 2010). This study found that TN and TP were lower than in the uncontaminated soil (0.44 and 1.07 g/kg). This may be due to nutrient consumption during the microbial biodegradation of TPH. As a result, the C/N and C/P ratios increased in the contaminated soil.

Loess lacks TN, but is relatively abundant with TP; significant soil erosion in the loess plateau region may decrease soil fertility with less TN. Therefore, petroleum contamination will lead to nutrient imbalances in the loess. The lack of nitrogen limited the organic contaminant biodegradation by indigenous microorganisms. Generally, efficient bacterial growth requires optimal C/N and C/P ratios of 10:1 and 30:1, respectively (Oudot and Dutrieux 1989). However, this study's results indicate that crude oil contamination was associated with suboptimal nutrient levels, with C/N at 18.97–32.63 and C/P at 6.90–10.59. Previous studies indicate that petroleum hydrocarbon degradation rates could be increased by adding supplemental nutrients, particularly nitrogen. This suggests that particular attention should be paid to nutrient adjustments before bioremediating oil-contaminated fields (Braddock et al. 1997).

Moisture is also a key factor influencing petroleum biodegradation. Usually, petroleum contamination lowers soil moisture, because petroleum hydrocarbon compounds absorbed on soil capillaries and pores make the soil more hydrophobic (Masakorala et al. 2014). In this study, the average soil moisture in the wasteland was 10.09%, which was significantly lower than in the farmland (average moisture of 22.00%). This may be because crop growth supports water conservation. Heavier petroleum contamination in the wasteland aggravates water loss. Furthermore, the Yanchang oilfield is in the drought/semi-drought loess plateau, where soil and water erosion naturally occurs. As such, soil water content is also a typical constraint impacting petroleum biodegradation in the loess plateau.

Stable carbon isotope composition and modified TPH

Table 3 shows the stable carbon isotope distribution in the soil samples collected from the wasteland adjacent to the oil wells. The $\delta^{13}C_{org}$ values represented the stable carbon isotopes in the samples' organic matter, and ranged from − 29.02 to − 24.67‰ in the contaminated soil samples. These ratios were significantly ($p < 0.01$) different from the levels in the samples derived from petroleum (− 32.02‰) and the background soil (− 23.03‰). The $\delta^{13}C_{org}$ values in the contaminated soil may have been slightly depleted by petroleum contributions. The $\delta^{13}C_{extra\text{-}org}$ value represents the ratio of stable carbon isotopes in the soil samples after extraction by dichloromethane; the

Table 3 Stable carbon isotope composition of organic compounds, partition coefficients, and the modified TPH in the wasteland soil adjacent to oil wells

Sample no.	Life of the adjacent oil well	$\delta^{13}C_{org}$ (‰)	$\delta^{13}C_{extra\text{-}org}$ (‰)	Partition coefficient		Modified TPH (mg/kg)
				X	X^a	
N-7	1991–2004	− 24.70	− 24.20	18.58	13.01	5937.59
N-6	1987–2014	− 25.33	− 24.30	21.91	14.13	5857.68
O-1	1992-	− 25.40	− 24.20	26.36	13.01	3173.07
O-2	2000-	− 26.40	− 25.29	37.82	25.14	6421.64
O-3	2007-	− 27.10	− 25.51	45.27	27.59	6639.42
O-4	2010-	− 29.02	− 25.80	66.63	30.81	6411.88
O-5	2015-	− 24.67	− 23.40	18.24	4.12	2238.66

[a] Petroleum: $\delta^{13}C_{org}$ = − 32.02‰. Background soil (B-15): $\delta^{13}C_{org}$ = −23.03‰

value was significantly lower in the contaminated samples compared to the uncontaminated background soil.

The wasteland sampling sites were adjacent to the oil wells in the loess plateau region. No other industries besides the petroleum industry contribute organic contaminants to the loess, and there are few plants on the wasteland. These conditions support the assumption that the organic carbon isotopes in the contaminated wasteland soil are derived solely from petroleum and the soil organic matter. The isotopic mass balance is presented as Eqs. (2) and (3):

$$\delta^{13}C_{\mathrm{contamnate-soil}} = X\delta^{13}C_{\mathrm{petroleum}} + (1-X)\delta^{13}C_{\mathrm{soil}} \tag{2}$$

$$\delta^{13}C_{\mathrm{extra-contamnate-soil}} = X^{*}\delta^{13}C_{\mathrm{petroleum}} + \left(1-X^{*}\right)\delta^{13}C_{\mathrm{soil}} \tag{3}$$

In this expression, $\delta^{13}C_{\mathrm{contamnate\text{-}soil}}$, $\delta^{13}C_{\mathrm{extra\text{-}contamnate\text{-}soil}}$, $\delta^{13}C_{\mathrm{petroleum}}$, and $\delta^{13}C_{\mathrm{soil}}$ are quantitative parameters characterizing, respectively, the ^{13}C isotope amount of total organic compounds in the contaminated soil, contaminated soil after being extracted by dichloromethane, petroleum, and the soil from the background area. X is the portion of petroleum-derived carbon and (1−X) is the portion of soil-derived carbon. X* is the portion of non-extractable petroleum-derived carbon, and (1−X*) is the portion of non-extractable soil-derived carbon.

Solving the equations for X, X* allows us to determine the portion of carbon derived from petroleum in the contaminated soil, and the petroleum residues that cannot be extracted with solvents. Then, the modified TPH (including both extractable and non-extractable TPH) is calculated using Eq. (4):

$$\text{Modified TPH} = \text{TPH} + \text{non}-\text{extractable TPH} \tag{4}$$

Using the definition of the parameters described above, Eq. (5) is derived as follows:

$$\frac{\text{Modified TPH}}{\text{Non}-\text{extractable TPH}} = \frac{X}{X^{*}} \tag{5}$$

Then, the modified TPH concentration is quantified by solving the two simultaneous Eqs. (4) and (5), resulting in Eq. (6):

$$\text{Modified TPH} = \left(\frac{X}{X-X^{*}}\right)\text{TPH} \tag{6}$$

Significantly, the modified TPH values obtained through $\delta^{13}C$ analysis were higher than the values measured using the gravimetric method (Tables 2 and 3). Gravimetric analysis has been a primary way to assess TPH concentrations and the petroleum contamination of soil (Mills et al. 1999); however, previous studies have found that this method has limited efficiency in extracting high molecular weight compounds (Douglas et al. 1992). As a result, some non-extractable fractions of petroleum in the soil are not measured using the typical gravimetric method.

Biodegradation has been assumed to dominate the long-term petroleum residual degradation process (Nocentini et al. 2000), and many studies (Huang et al. 1997; Mazeas et al. 2002; Sun et al. 2005) have demonstrated that there is no carbon isotope fractionation in hydrocarbon biodegradation. In addition, there was a markedly different $\delta^{13}C$ between the uncontaminated soil (− 23.030‰) and the petroleum (− 32.015‰). Therefore, the $\delta^{13}C$ value of contaminated soil can serve as a specific marker to evaluate the extent of petroleum contamination. Using $\delta^{13}C$ to derive the modified TPH concentration more precisely evaluates soil petroleum contamination. Results suggest that that the contamination in the study area was more significant than indicated by extraction gravimetric analysis.

In addition, according to the isotopic mass balance, the partition coefficients of total petroleum (X) and non-extractable petroleum (X*) in the contaminated soils were calculated using Eqs. (2) and (3). With the exception of sample O-5 (2015–), the X and X* values of the samples adjacent to the active wells (X, 25.83–66.67; X*, 21.69–30.52) were significantly higher than for the samples collected near non-working wells (X, 25.62–25.82; X*, 13.91–14.13).

Among the sampling sites near the active oil wells (again, excluding sample O-5), X and X* values significantly decreased as the duration of oil well use increased. The X value of 66.67 for sample O-4 (2010–) dropped to 25.83 of the sample for sample O-1 (1992–). The X* value of 30.52 for sample O-4 (2010–) dropped to 21.69 for sample O-1 (1992–). These results show that X decreased at a faster rate than X*.

Nevertheless, sample O-5 (2015–) had relatively high $\delta^{13}C_{\mathrm{org}}$ and $\delta^{13}C_{\mathrm{extra\text{-}org}}$ values compared to other samples. This resulted in a lower X and X*. This may have resulted from the introduction of some other stable carbon isotope, besides petroleum and soil. As a newly established well, the land near this sampling point was a newly established wasteland; as such, the plant biomass residue in the soil may contribute to the higher $\delta^{13}C$ value.

This study showed that the $\delta^{13}C_{\mathrm{extra\text{-}org}}$ levels in the contaminated samples were generally lower than levels found in background soil (− 23.03‰), indicating there were non-extricable petroleum residues in the contaminated soil samples (Table 3). Based on the variation in partition coefficients X and X* with respect to contamination history, the total petroleum and non-extractable fractions of petroleum in the contaminated soil gradually decreased over time. Non-extractable petroleum fractions (X*) declined less than the total petroleum (X) did. This suggests that the non-extricable petroleum residues were more difficult to degrade than other petroleum components.

Table 4 Concentration of n-alkanes and their geochemical indices in different samples collected in Yanchang oilfield, China

Parameter	Geochemical indices of samples													
	Wasteland adjacent to oil wells							Farmland		River sediment				Petroleum
	O-1	O-2	O-3	O-4	O-5	N-6	N-7	FL-8	FL-9	S-10	S-11	S-12	S-13	P-14
Σ n-alkanes (μg/g)	32.46	60.19	107.27	140.65	22.86	18.73	13.32	13.91	16.57	12.91	36.39	27.99	31.45	/
LMW/HMW	0.99	0.51	0.88	0.77	0.95	0.93	1.45	0.23	0.71	0.85	1.20	0.99	1.94	0.90
$CPI_{13–35}$	1.09	1.13	1.07	1.06	1.05	1.10	1.03	1.06	1.05	1.15	1.20	0.94	1.48	1.08
$CPI_{13–22}$	1.08	1.15	1.09	1.01	1.06	1.24	1.03	1.18	1.05	1.08	1.05	0.78	1.18	1.11
$CPI_{23–35}$	1.39	1.28	1.35	1.38	1.33	1.23	1.42	1.19	1.35	1.35	1.71	1.26	2.81	1.43
MH	n-C_{27}	n-C_{29}	n-C_{26}	n-C_{27}	n-C_{26}	n-C_{26}	n-C_{19}	n-C_{27}	n-C_{26}	n-C_{16}	n-C_{16}	n-C_{16}	n-C_{16}	n-C_{27}
n-C_{17}/Pr	2.16	2.07	1.25	1.39	2.33	2.61	2.60	2.12	1.97	2.30	2.75	7.13	2.59	3.24
n-C_{18}/Ph	1.83	1.58	1.03	1.40	2.07	1.79	2.50	1.78	1.35	1.52	2.22	6.57	1.95	3.81
Pr/Ph	0.81	0.84	0.76	0.76	0.82	0.85	0.80	0.56	0.70	0.84	0.86	0.83	0.93	0.92

LMW/HMW sum of LMW n-alkanes (n-C_{13}~n-C_{23}) over sum of HMW n-alkanes (n-C_{23}~n-C_{35}), *$CPI_{13–35}$* odd to even carbon preference index from n-C_{13} to n-C_{35}, *$CPI_{13–22}$* odd to even carbon preference index from n-C_{13} to n-C_{22}, *$CPI_{23–35}$* odd to even carbon preference index from n-C_{23} to n-C_{35}, *MH* major hydrocarbon, *n-C_{17}/Pr* ratio of C_{17} n-alkane to pristane, *n-C_{18}/P* ratio of C_{18} n-alkane to phytane, *Pr/Ph* ratio of pristane to phytane

Concentration and geochemical indices of n-alkanes, PAHs

Investigating n-alkanes and PAHs confirmed the petroleum contamination in Yanchang oilfield. The total (Σ) alkanes and PAHs of the contaminated samples varied from 12.91 to 140.65 mg/kg and from 103.59 to 563.50 μg/kg, respectively (Tables 4 and 5); the background values were below the MQL. The n-alkane concentrations (Table S4) observed in this study did not significantly differ from levels seen in surface soils of the Hunpu wastewater-irrigated area in northeast China (14.34–55.37 mg/kg) (Zhang et al. 2012).

The USEPA has classified 16 PAHs as priority pollutants; they are often targeted during environmental sampling and testing. Table 5 shows that the total concentration of the 16 PAHs in this study (103.59–563.50 μg/kg) was higher than concentrations detected in the Beiluohe River region in northern Shaanxi (17.7–407.7 μg/kg) (Zhang et al. 2007). However, the concentration was lower than others detected at long-term industrial areas in developed countries, such as near New Orleans, Louisiana, in the USA (647–40,962 μg/kg) and in the Seine River Basin in France (3390–5690 μg/kg) (Mielke et al. 2004; Motelay-Massei et al. 2004).

Table 4 lists the N-alkane distribution indices, including LMW/HMW, CPI, n-C_{17}/Pr, n-C_{18}/Ph, and Pr/Ph. The LMW/HMW values were generally less than 1, with the exception of samples N7 (LMW/HMW = 1.45), S-11 (LMW/HMW = 1.20), and S-13 (LMW/HMW = 1.94). Samples from the farmland had a lower LMW/HMW value (0.23, 0.71).

Typically, abundant high-carbon number hydrocarbons, accompanied by a small number of low-carbon number hydrocarbons, indicates heavy petroleum contamination and degradation (Colombo et al. 1989). In this study, lighter-end n-alkanes (n-C_9 to n-C_{12}) were not detected because of the weathering processes (Sharma et al. 2002). When petroleum and its derivatives have many low or high molecular weight hydrocarbons, they can interfere with LMW/HMW values (de Oliveira and dos Santos Madureira 2011). Because lower molecular weight n-alkanes preferentially biodegrade over relatively higher molecular weight n-alkane compounds, LMW/HMW can be used to recognize the extent of petroleum degradation (Coulon et al. 2004; Sanscartier et al. 2009). The LMW/HMW ratio is usually close to 1 in petroleum products (Tran et al. 1997). LMW/HMW ratios lower than 1 indicate possibly heavy petroleum contamination and degradation in soil (Zhang et al. 2012).

In this study, the LMW/HMW of samples O-1 (0.99), O-5 (0.95), and S-12 (0.99) approached one (1), suggesting a recent influx of fresh oil (Wang et al. 2006). Lower LMW/HMW levels were found in samples O-2 (0.51), O-3 (0.88), O-4 (0.77), N-6 (0.93), F-8 (0.23), F9 (0.71), and S-10 (0.85). This suggests that higher LMW n-alkane biodegradation occurred at these sites (Stout et al. 2002). A higher LMW/HMW was found in sample N-7 (1.45) adjacent to a waste oil well that had been used a long time (1992–2004). This result is consistent with Chang et al. (2010), who found that higher molecular weight alkanes can be degraded from aged contaminated soils by stimulating indigenous microorganisms in cold climates. The higher molecular weight alkane biodegradation in aged contaminated soil can also be confirmed by the MH of sample N-7 as n-C_{19}. The higher LMW/HMW of samples S-11 (1.20) and S-13 (1.94) can be attributed to the continuous input of fresh petroleum (Wang et al. 2006).

CPI is defined as the ratio of odd to even carbon-numbered n-alkanes. Usually, CPI values near 1 indicate petroleum inputs (Petersen et al. 2007); higher CPI values, mostly between

Table 5 Concentrations of 16 US EPA PAHs in different samples collected in Yanchang oilfield, China

Compounds	PAH concentrations in samples (μg/kg)												
	Wasteland adjacent to oil wells							Farmland		River sediment			
	O-1	O-2	O-3	O-4	O-5	N-6	N-7	FL-8	FL-9	S-10	S-11	S-12	S-13
Naphthalene	<MOL	<MOL	<MOL	<MOL	<MOL	<MOL	<MOL	<MOL	<MOL	<MOL	<MOL	<MOL	<MOL
Acenaphthene	<MOL	<MOL	<MOL	<MOL	<MOL	<MOL	<MOL	<MOL	<MOL	<MOL	<MOL	<MOL	<MOL
Acenaphthylene	<MOL	<MOL	<MOL	<MOL	<MOL	<MOL	<MOL	<MOL	<MOL	<MOL	<MOL	<MOL	<MOL
Fluorene	8.41	12.58	9.55	11.58	6.73	8.78	2.79	8.52	2.02	3.63	5.12	16.31	11.83
Anthracene	3.73	5.57	2.85	4.52	2.59	4.47	1.72	2.38	1.55	1.39	2.01	2.31	6.98
Phenanthrene	59.50	97.25	54.70	67.16	48.88	70.02	33.41	63.75	35.01	27.82	26.52	117.44	61.91
Fluoranthene	23.55	78.25	8.57	11.06	7.52	21.77	8.34	11.64	6.01	5.49	6.37	7.21	22.07
Pyrene	29.70	79.67	19.02	28.49	20.39	32.13	8.98	11.29	15.77	7.67	8.36	8.84	22.73
Benz[a]anthracene	10.05	18.96	3.67	4.61	4.07	11.67	6.55	3.87	3.23	5.61	5.43	4.85	14.26
Chrysene	28.01	64.98	12.62	68.17	13.60	60.70	13.61	10.81	32.51	10.76	12.73	12.96	49.64
Benzo[b]fluoranthene	20.81	47.14	14.60	39.52	10.10	41.48	4.59	9.76	14.95	11.11	7.42	11.35	39.56
Benzo[k]fluoranthene	11.02	20.45	9.08	19.87	10.89	20.08	7.90	5.09	9.07	5.33	10.98	4.09	13.77
Benzo[a]pyrene	18.30	51.95	16.01	41.78	9.36	46.75	8.82	4.71	11.08	8.59	8.86	7.74	29.19
Indeno[1,2,3-cd]pyrene	5.19	33.01	3.28	8.77	3.72	8.80	2.73	3.07	3.97	4.30	5.39	4.64	12.33
Benzo[ghi]perylene	9.33	46.64	5.75	11.03	4.67	22.86	5.16	2.99	6.46	5.99	7.80	5.73	21.26
Dibenz[a,h]anthracene	5.91	7.05	5.50	6.94	5.50	9.37	5.41	3.08	6.07	5.89	6.12	5.83	8.84
Σ PAHs	233.50	563.50	165.20	323.25	148.03	358.87	110.01	140.97	147.70	103.59	113.11	209.29	314.37
Phe/Ant	15.97	17.45	19.19	14.85	18.88	15.68	19.44	26.73	22.59	20.05	13.20	50.91	8.87
Fluor/Pyr	0.79	0.98	0.45	0.39	0.37	0.68	0.93	1.03	0.38	0.72	0.76	0.82	0.97

Σ PAHs = sum of 16 US EPA PAHs, Phe/Ant = phenanthrene/anthracene, Fluor/Pyr = fluoranthene/pyrene, MOL = method quantification limit

3 and 6, indicate that the hydrocarbons originated from vascular plant epicuticular wax (Boehm and Requejo 1986). In this study, CPI values in the contaminated soil were slightly higher than 1 (CPI_{13-35}, 1.03–1.10; CPI_{13-22}, 1.01–1.24; CPI_{22-35}, 1.19–1.42). This confirmed the dominance of petrogenic hydrocarbons, with minor biogenic hydrocarbons, in the soil (Zheng and Richardson 1999). However, CPI values in the sediment samples were more complicated. The CPI of sample S-12 was lower than 1: CPI_{13-35} was 0.99, CPI_{13-22} was 0.94, and CPI_{23-35} was 0.78. In comparison, samples S-10, S-11, and S-13 had higher CPI values. The CPI_{23-35} of sample S-11 was 1.71; the CPI_{23-35} of sample S-13 was 2.81. The lower CPI demonstrated that n-alkanes in sample S-12 are mainly due to anthropogenic inputs, whereas the higher CPI in samples S-11 and S-13 may be due to hydrocarbons from aquatic biomass (Tanner et al. 2010).

The ratios of n-alkanes over acyclic isoprenoid alkanes (i.e., n-C_{17}/Pr and n-C_{18}/Ph) and the Pr/Ph ratio can be used to identify petroleum sources and assess weathering. The presence of the isoprenoids (Pr and Ph) confirmed petroleum contamination in the Yanchang oilfield. All samples except sample S-12 had a lower n-C_{17}/Pr (1.25 to 2.60) and n-C_{18}/Pr (1.03–2.22) than petroleum (n-C_{17}/Pr as 3.24, n-C_{18}/Pr as 3.81). With the exception of sample S-13 (0.93), the Pr/Ph ratios in the contaminated sediments (0.83–0.86) were also lower than in petroleum (0.92). Acyclic isoprenoid alkanes degrade with more difficulty than n-alkanes. As such, a lower Pr/Ph ratio indicates more petroleum degradation in the contaminated soil than in soil that is more freshly contaminated (da Silva and Bicego 2010; Gao et al. 2007).

Pyrolytic PAHs are usually characterized by the dominance of parent compounds with four or more aromatic rings. In contrast, petrogenic PAHs are characterized by an abundance of two to three aromatic ring compounds (Soclo et al. 2000). Therefore, some molecular ratios, such as phenanthrene/anthracene (Phe/Ant) and fluoranthene/pyrene (Fluor/Pyr), have been used to distinguish petrogenic (petroleum) and pyrolytic contamination sources (petroleum and biomass combustion). A Fluor/Pyr ratio of less than 1 indicates petrogenic inputs; a ratio greater than 1 indicates pyrolytic sources (Baumard et al. 1998). A Phe/Ant ratio that is higher than 10 generally indicates petrogenic inputs, whereas a Phe/Ant ratio less than 10 is typical of pyrolytic sources (Budzinski et al. 1997; Soclo et al. 2000).

In this study, with the exception of samples FL-8 (Fluor/Pyr = 1.03) and S-13 (Phe/Ant = 8.84), the Fluor/Pyr ratios (0.38 to 0.98) were less than 1. Phe/Ant ratios (14.85–50.91) were higher than 10 (Table 5). Phenanthrene concentrations were the highest of all the PAHs in all samples, including the petroleum sample. This points to a petrogenic input into the thermodynamically stable structure (Baumard et al. 1998), and suggests that petrogenic PAHs dominate most samples. Given significant regional soil erosion, it is vital to consider the potential risks that PAHs pose to nearby agricultural and aquatic ecosystems.

An unresolved complex mixture (UCM) was detected at all contaminated sampling sites (Fig. S1). UCM is composed of alkylated and cyclic compounds, which the GC is not able to discriminate; as such, they appear as a hump in GC chromatograms (Companioni Damas et al. 2009). UCM accumulation is believed to result from long-term petroleum residual degradation (Mills et al. 1999). Further, all samples contained almost identical distributions of steranes and triterpanes, typical for petroleum (Fig. S2 and Fig. S3). Terpanes and steranes are ubiquitous in petroleum, and resist biodegradation.

These results indicate high and persistent petroleum inputs to soil and river sediment in the Yanchang oilfield. Biodegradation dominated the petroleum's long-term residual degradation process; the distribution of different n-alkanes appears to align with the age of petroleum contamination, environmental conditions, and the indigenous biomass.

Conclusion

There is significant petroleum contamination in the loess of the Yanchang oilfield. Tests using $\delta^{13}C$ to detect modified TPH found more significant contamination, compared to testing done using extraction gravimetric analysis. Soil erosion in the study area has resulted in petroleum contamination spreading to other ecosystems, including nearby farmlands and rivers. This could create hazards for human beings. Petroleum weathering occurred at each sampling site, resulting in the partial attenuation of saturates, the slight accumulation of aromatics, and apparent accumulation of polar components. "Chemical fingerprint" indicators further confirmed that heavy petroleum contamination and degradation occurred in the study area. Weathered oil residues in soil, accumulated over long periods, may cause nutrient imbalances and unsuitable pH and moisture conditions for microbial metabolic activities. This petroleum contamination investigation provides critical insights that can inform site-specific remediation techniques.

Acknowledgements This work was supported by the National Natural Science Foundation of China (Grant No. 31670510), Funding of State Key Laboratory of Loess and Quaternary Geology in China (Grant No. SKLLQG), and the Fundamental Research Funds for the Central Universities in China.

References

Atlas RM, Hazen TC (2011) Oil biodegradation and bioremediation: a tale of the two worst spills in US history. Environ Sci Technol 45: 6709–6715

Bauder TA, Barbarick KA, Ippolito JA, Shanahan JF, Ayers PD (2005) Soil properties affecting wheat yields following drilling-fluid application. J Environ Qual 34:1687–1696

Baumard P, Budzinski H, Michon Q, Garrigues P, Burgeot T, Bellocq J (1998) Origin and bioavailability of PAHs in the Mediterranean sea from mussel and sediment records. Estuar Coast Shelf Sci 47:77–90

Boehm PD, Requejo AG (1986) Overview of the recent sediment hydrocarbon geochemistry of Atlantic and gulf-coast outer continental-shelf environments. Estuar Coast Shelf Sci 23:29–58

Braddock JF, Ruth ML, Catterall PH, Walworth JL, McCarthy KA (1997) Enhancement and inhibition of microbial activity in hydrocarbon-contaminated arctic soils: implications for nutrient-amended bioremediation. Environ Sci Technol 31:2078–2084

Budzinski H, Jones I, Bellocq J, Pierard C, Garrigues P (1997) Evaluation of sediment contamination by polycyclic aromatic hydrocarbons in the Gironde estuary. Mar Chem 58:85–97

Chang W, Dyen M, Spagnuolo L, Simon P, Whyte L, Ghoshal S (2010) Biodegradation of semi- and non-volatile petroleum hydrocarbons in aged, contaminated soils from a sub-Arctic site: laboratory pilot-scale experiments at site temperatures. Chemosphere 80:319–326

Colombo JC, Pelletier E, Brochu C, Khalil M, Catoggio JA (1989) Determination of hydrocarbon sources using n-alkane and polyaromatic hydrocarbon distribution indexes—case-study—Rio-de-la-Plata estuary, Argentina. Environ Sci Technol 23:888–894

Companioni Damas EY, Cora Medina MO, Nunez Clemente AC, Diaz Diaz MA, Gonzalez Bravo L, Marbot Ramada R, Montes de Oca Porto R (2009) Validation of an analytical methodology for the quantitative analysis of petroleum hydrocarbons in marine sediment samples. Quim Nova 32:855–U35

Coulon F, Pelletier E, St Louis R, Gourhant L, Delille D (2004) Degradation of petroleum hydrocarbons in two sub-Antarctic soils: influence of an oleophilic fertilizer. Environ Toxicol Chem 23: 1893–1901

da Silva DAM, Bicego MC (2010) Polycyclic aromatic hydrocarbons and petroleum biomarkers in Sao Sebastiao Channel, Brazil: assessment of petroleum contamination. Mar Environ Res 69:277–286

de Oliveira CR, dos Santos Madureira LA (2011) Assessment and sources of nonaromatic hydrocarbons in surface sediments of three harbors in Santa Catarina State, Brazil. Environ Monit Assess 173: 91–105

Douglas GS, McCarthy KJ, Dahlen DT, Seavey JA, Steinhauer WG, Prince RC, Elmendorf DL (1992) The use of hydrocarbon analyses for environmental assessment and remediation. J Soil Contam 1: 197–216

Douglas GS, Bence AE, Prince RC, McMillen SJ, Butler EL (1996) Environmental stability of selected petroleum hydrocarbon source and weathering ratios. Environ Sci Technol 30:2332–2339

Fedorak PM, Westlake DWS (1981) Degradation of aromatics and saturates in crude-oil by soil enrichments. Water Air Soil Pollut 16:367–375

Gao X, Chen S, Xie X, Long A, Ma F (2007) Non-aromatic hydrocarbons in surface sediments near the Pearl River estuary in the South China Sea. Environ Pollut 148:40–47

Gianfreda L, Rao MA, Piotrowska A, Palumbo G, Colombo C (2005) Soil enzyme activities as affected by anthropogenic alterations: intensive agricultural practices and organic pollution. Sci Total Environ 341:265–279

Havelcova M, Melegy A, Rapant S (2014) Geochemical distribution of polycyclic aromatic hydrocarbons in soils and sediments of El-Tabbin, Egypt. Chemosphere 95:63–74

Huang J, Shi Y, Zeng G, Gu Y, Chen G, Shi L, Hu Y, Tang B, Zhou J (2016) Acyl-homoserine lactone-based quorum sensing and quorum quenching hold promise to determine the performance of biological wastewater treatments: an overview. Chemosphere 157:137–151

Huang Y, Eglinton G, Ineson P, Latter PM, Bol R, Harkness DD (1997) Absence of carbon isotope fractionation of individual n-alkanes in a 23-year field decomposition experiment with Calluna vulgaris. Org Geochem 26:497–501

Karvelas M, Katsoyiannis A, Samara C (2003) Occurrence and fate of heavy metals in the wastewater treatment process. Chemosphere 53: 1201–1210

Koponen HT, Jaakkola T, Keinanen-Toivola MM, Kaipainen S, Tuomainen J, Servomaa K, Martikainen PJ (2006) Microbial communities, biomass, and activities in soils as affected by freeze thaw cycles. Soil Biol Biochem 38:1861–1871

Labud V, Garcia C, Hernandez T (2007) Effect of hydrocarbon pollution on the microbial properties of a sandy and a clay soil. Chemosphere 66:1863–1871

Lauber CL, Hamady M, Knight R, Fierer N (2009) Pyrosequencing-based assessment of soil pH as a predictor of soil bacterial community structure at the continental scale. Appl Environ Microbiol 75: 5111–5120

Leahy JG, Colwell RR (1990) Microbial-degradation of hydrocarbons in the environment. Microbiol Rev 54:305–315

Liang Y, Zhang X, Wang J, Li G (2012) Spatial variations of hydrocarbon contamination and soil properties in oil exploring fields across China. J Hazard Mater 241:371–378

Mao D, Lookman R, Van De Weghe H, Weltens R, Vanermen G, De Brucker N, Diels L (2009) Estimation of ecotoxicity of petroleum hydrocarbon mixtures in soil based on HPLC-GCXGC analysis. Chemosphere 77:1508–1513

Masakorala K, Yao J, Chandankere R, Liu H, Liu W, Cai M, Choi MMF (2014) A combined approach of physicochemical and biological methods for the characterization of petroleum hydrocarbon-contaminated soil. Environ Sci Pollut Res 21:454–463

Mazeas L, Budzinski H, Raymond N (2002) Absence of stable carbon isotope fractionation of saturated and polycyclic aromatic hydrocarbons during aerobic bacterial biodegradation. Org Geochem 33: 1259–1272

Mielke HW, Wang GD, Gonzales CR, Powell ET, Le B, Quach VN (2004) PAHs and metals in the soils of inner-city and suburban New Orleans, Louisiana, USA. Environ Toxicol Pharmacol 18: 243–247

Mills MA, McDonald TJ, Bonner JS, Simon MA, Autenrieth RL (1999) Method for quantifying the fate of petroleum in the environment. Chemosphere 39:2563–2582

Motelay-Massei A, Ollivon D, Garban B, Teil MJ, Blanchard M, Chevreuil M (2004) Distribution and spatial trends of PAHs and PCBs in soils in the Seine River basin, France. Chemosphere 55: 555–565

Nocentini M, Pinelli D, Fava F (2000) Bioremediation of a soil contaminated by hydrocarbon mixtures: the residual concentration problem. Chemosphere 41:1115–1123

Oudot J, Dutrieux E (1989) Hydrocarbon weathering and biodegradation in a tropical Estuarine ecosystem. Mar Environ Res 27:195–213

Peng S, Zhou Q, Cai Z, Zhang Z (2009) Phytoremediation of petroleum contaminated soils by Mirabilis Jalapa L. in a greenhouse plot experiment. J Hazard Mater 168:1490–1496

Petersen HI, Nytoft HP, Ratanasthien B, Foopatthanakamol A (2007) Oils from Cenozoic rift-basins in central and northern Thailand: source and thermal maturity. J Pet Geol 30:59–77

Quatrini P, Scaglione G, De Pasquale C, Riela S, Puglia AM (2008) Isolation of Gram-positive n-alkane degraders from a hydrocarbon-contaminated Mediterranean shoreline. J Appl Microbiol 104:251–259

Salanitro JP, Dorn PB, Huesemann MH, Moore KO, Rhodes IA, Jackson LMR, Vipond TE, Western MM, Wisniewski HL (1997) Crude oil hydrocarbon bioremediation and soil ecotoxicity assessment. Environ Sci Technol 31:1769–1776

Sanscartier D, Laing T, Reimer K, Zeeb B (2009) Bioremediation of weathered petroleum hydrocarbon soil contamination in the Canadian High Arctic: laboratory and field studies. Chemosphere 77:1121–1126

Sarkar D, Ferguson M, Datta R, Birnbaum S (2005) Bioremediation of petroleum hydrocarbons in contaminated soils: comparison of biosolids addition, carbon supplementation, and monitored natural attenuation. Environ Pollut 136:187–195

Sharma VK, Hicks SD, Rivera W, Vazquez FG (2002) Characterization and degradation of petroleum hydrocarbons following an oil spill into a coastal environment of south Texas, USA. Water Air Soil Pollut 134:111–127

Shi Y, Huang J, Zeng G, Gu Y, Chen Y, Yi H, Bi T, Zhou J, Ying Y, Shi L (2017) Exploiting extracellular polymeric substances (EPS) controlling strategies for performance enhancement of biological wastewater treatments: an overview. Chemosphere 180:396–411

Soclo HH, Garrigues P, Ewald M (2000) Origin of polycyclic aromatic hydrocarbons (PAHs) in coastal marine sediments: case studies in Cotonou (Benin) and Aquitaine (France) areas. Mar Pollut Bull 40: 387–396

Stout SA, Uhler AD, Mccarthy KJ, Emsbo-Mattingly S (2002): Chemical fingerprinting of hydrocarbons. 137–260

Sun F-H, Zhou Q-X (2007) Metal accumulation in the polychaete Hediste japonica with emphasis on interaction between heavy metals and petroleum hydrocarbons. Environ Pollut 149:92–98

Sun YG, Chen ZY, SP X, Cai PX (2005) Stable carbon and hydrogen isotopic fractionation of individual n-alkanes accompanying biodegradation: evidence from a group of progressively biodegraded oils. Org Geochem 36:225–238

Tanner BR, Uhle ME, Mora CI, Kelley JT, Schuneman PJ, Lane CS, Allen ES (2010) Comparison of bulk and compound-specific delta C-13 analyses and determination of carbon sources to salt marsh sediments using n-alkane distributions (Maine, USA). Estuarine Coastal and Shelf. Science 86:283–291

Teng Y, Zhou Q, Miao X, Chen Y (2015) Assessment of soil organic contamination in a typical petrochemical industry park in China. Environ Sci Pollut Res 22:10227–10234

Tran K, CC Y, Zeng EY (1997) Organic pollutants in the coastal environment off San Diego, California .2. Petrogenic and biogenic sources of aliphatic hydrocarbons. Environ Toxicol Chem 16:189–195

Wang X, Feng J, Zhao J (2010) Effects of crude oil residuals on soil chemical properties in oil sites, Momoge Wetland, China. Environ Monit Assess 161:271–280

Wang Y, Feng J, Lin Q, Lyu X, Wang X, Wang G (2013) Effects of crude oil contamination on soil physical and chemical properties in Momoge wetland of China. Chin Geogr Sci 23:708–715

Wang Z, Stout SA, Fingas M (2006) Forensic fingerprinting of biomarkers for oil spill characterization and source identification. Environ Forensic 7:105–146

Wang Z, Yang C, Yang Z, Hollebone B, Brown CE, Landriault M, Sun J, Mudge SM, Kelly-Hooper F, Dixon DG (2012) Fingerprinting of petroleum hydrocarbons (PHC) and other biogenic organic compounds (BOC) in oil-contaminated and background soil samples. J Environ Monit 14:2367–2381

Zhang J, Wang R, Du X, Li F, Dai J (2012) Characterization of contamination, source and degradation of petroleum between upland and paddy fields based on geochemical characteristics and phospholipid fatty acids. J Environ Sci 24:1995–2003

Zhang L, Shi K, Yue L (2007) Chemical characteristics and pollution sources of petroleum hydrocarbons and PAHs in sediments from the Beiluohe River, Northern China. Environ Geol 53:307–315

Zheng GJ, Richardson BJ (1999) Petroleum hydrocarbons and polycyclic aromatic hydrocarbons (PAHs) in Hong Kong marine sediments. Chemosphere 38:2625–2632

Zhou Q, Cai Z, Zhang Z, Liu W (2011) Ecological remediation of hydrocarbon contaminated soils with weed plant. J Resour Ecol 2:97–105

Ziakun AM, Brodskii ES, Baskunov BP, Zakharchenko VN, Peshenko VP, Filonov AE, Vetrova AA, Ivanova AA, Boronin AM (2014) Bioremediation of oil-polluted soils: using the 13C / 12C ratio to characterize microbial products of oil hydrocarbon biodegradation. Prikl Biokhim Mikrobiol 50:497–507